Quantifying the Effect of Burial of Amino Acid Residues on Protein Stability

Hongyi Zhou and Yaoqi Zhou*
Howard Hughes Medical Institute Center for Single Molecule Biophysics, Department of Physiology and Biophysics, State University of New York at Buffalo, Buffalo, New York

ABSTRACT **The average contribution of individual residue to folding stability and its dependence on buried accessible surface area (ASA) are obtained by two different approaches. One is based on experimental mutation data, and the other uses a new knowledge-based atom–atom potential of mean force. We show that the contribution of a residue has a significant correlation with buried ASA and the regression slopes of 20 amino acid residues (called the buriability) are all positive (pro-burial). The buriability parameter provides a quantitative measure of the driving force for the burial of a residue. The large buriability gap observed between hydrophobic and hydrophilic residues is responsible for the burial of hydrophobic residues in soluble proteins. Possible factors that contribute to the buriability gap are discussed. Proteins 2004;54:315–322.**

Key words: hydrophobicity scale; knowledge-based potential; buriability; stability scale

INTRODUCTION

The aim of this work is to assess how individual residues contribute to the stability of proteins. In the hydrophobic model of stability, hydrophobic interaction is believed to be the main driving force that stabilizes the native structures of proteins.[1,2] In this model, the contribution of a residue to stability (the stability scale) is assumed to follow the hydrophobicity scales obtained from oil-to-water free-energy transfer experiments. These experiments suggested that the contributions of hydrophilic residues to stability should be marginal or negative, compared with those of hydrophobic residues, and hydrophobicity drives the burial of hydrophobic residues in the interior of soluble proteins. On the other hand, the packing model of stability[3–5] proposes that the burial of either hydrophilic or hydrophobic residues inside proteins makes similar contribution. To shed new light on this fundamental issue, we derived the stability scales of amino acid residues from a large mutation database ($\overline{\Delta G}_m$) and from an atom–atom potential of mean force (APMF) based on a new Distance-scaled, Finite Ideal-gas REference (DFIRE) state[6] ($\overline{\Delta G}_s$). The results suggest a new concept of buriability that provides a quantitative measure of the driving force for the burial of an amino acid residue in proteins.

RESULTS

We first performed correlation analysis among the new stability scales ($\overline{\Delta G}_m$and $\overline{\Delta G}_s$) and oil-to-water transfer free energy scales that are shown in Table I. The correlation coefficients between $\overline{\Delta G}_m$ and $\overline{\Delta G}_s$ are 0.91, 0.93, and 0.79 for all, hydrophobic, and hydrophilic residues, respectively. The significant correlation indicates the overall agreement between two different approaches and provides a cross-validation of the two approaches.

The hydrophobic-residue portions of the new scales are correlated strongly with many transfer scales. For example, the correlation coefficient (R) for 10 hydrophobic residues is 0.95 between $\overline{\Delta G}_s$ and $\Delta G_{\mathrm{octanol}}$, the octanol-to-water transfer free energy[7] corrected with an additional Flory–Huggins molar-volume term.[8] This finding validates the stability scales derived from APMF and the mutation database as well as the use of transfer experiments of hydrophobic residues to interpret mutation-induced change in stability.[9] However, the hydrophilic-residue portion of $\overline{\Delta G}_s$ (or $\overline{\Delta G}_m$), does not correlate significantly with any oil-to water transfer scales. An example is shown in Figure 1. Instead, the hydrophilic portion and the entire scale are correlated significantly with the average buried solvent accessible surface area (ASA) A^0–<A> (Fig. 2). The correlation coefficients between $\overline{\Delta G}_s$ and A^0–<A> are 0.95, 0.95, and 0.92 for all 19 residues (except Cys; see Fig. 2 caption), hydrophobic residues, and hydrophilic residues, respectively. The correlation coefficients between $\overline{\Delta G}_m$ and A^0–<A> are 0.96, 0.96, and 0.84, for all 20 residues, hydrophobic residues, and hydrophilic residues, respectively. This finding validates the use of the average buried ASA as a "hydrophobicity" scale.[10,11]. The previous use of A^0–<A> was largely due to its correlation with the oil-to-water transfer experiments of hydrophobic residues.

The dependence of $\Delta G_s(I)$ from APMF on burial ASA is generally linear for all 20 amino acid residues. (R = 0.79

Grant sponsor: National Institutes of Health; Grant numbers: GM 066049 and 068530; Grant sponsor: HHMI to SUNY Buffalo; Grant sponsor: Center for Computational Research and the Keck Center for Computational Biology at SUNY Buffalo.

*Correspondence to: Dr. Yaoqi Zhou, Howard Hughes Medical Institute Center for Single Molecule Biophysics and Department of Physiology and Biophysics, State University of New York at Buffalo, 124 Sherman Hall, Buffalo, NY 14214. E-mail: yqzhou@buffalo.edu

Received 19 May 2003; Accepted 26 June 2003

TABLE I. The Stability Scales, Buriability, and Average Buried Accessible Surface Area of 20 Amino Acid Residues

Residue name	$\overline{\Delta G_s}^a$ (kcal/mol)	$\overline{\Delta G_m}^b(\sigma^e)$ (kcal/mol)	$A^0 - <A>^c$ (Å^2)	$\Delta G_{\text{octanol}}{}^d$ (kcal/mol)	Buriability (σ^e) (cal/mol/Å^2)
TRP[f]	6.46	5.64(0.34)	226	7.14	24.5 (1.5)
TYR[f]	5.01	4.46(0.14)	192	4.90	19.5 (1.3)
PHE[f]	5.88	4.84(0.15)	193	6.03	23.9 (1.5)
ILE[f]	4.50	4.59(0.11)	170	5.87	20.3 (1.7)
LEU[f]	4.71	4.72(0.11)	171	5.89	20.8 (1.5)
MET[f]	3.63	3.91(0.15)	182	4.80	15.7 (1.6)
VAL[f]	3.77	3.67(0.11)	146	4.51	19.5 (1.9)
ALA[f]	2.18	1.79(0.09)	97	2.03	13.4 (2.6)
CYS[f]	3.89	2.22(0.19)	78	4.19	22.6 (4.3)
GLY[f]	1.17	0.70(-)	64	1.01	7.0 (4.1)
HIS	2.51	3.06(0.20)	144	2.95	11.3 (1.5)
ARG	2.71	3.20(0.20)	150	1.78	8.5 (1.0)
GLN	2.16	2.37(0.18)	119	2.48	8.5 (1.4)
GLU	1.89	2.52(0.14)	110	1.78	7.3 (1.4)
THR	2.18	2.45(0.12)	107	2.53	10.3 (2.0)
ASN	1.85	2.83(0.16)	103	1.40	7.6 (1.7)
LYS	2.12	2.50(0.14)	109	2.01	6.1 (1.1)
PRO	2.09	2.45(0.17)	95	3.51	9.9 (1.9)
ASP	1.75	2.33(0.14)	95	1.09	8.2 (1.8)
SER	1.66	1.82(0.13)	87	1.59	8.2 (2.5)

[a]The stability scale from the knowledge-based atom–atom potential.
[b]The relative stability scale extracted from mutation experiments. Because this is a relative scale, the scale is shifted by a constant value of 0.703 kcal/mol so that the average of $\overline{\Delta G_m}$ is the same as that of $\overline{\Delta G_s}$. The correlation coefficients between $\overline{\Delta G_m}$ and $\overline{\Delta G_s}$ are 0.91, 0.93, and 0.79 for all, hydrophobic, and hydrophilic residues, respectively. However, the hydrophilic-residue portion of $\overline{\Delta G_m}$ has no significant correlation with that of the stability scales based on the octanol scale ($R = 0.14$), other knowledge-based potentials,[38] and contact energies.[39]
[c]A^0 is from Ref. [36]. $<A>$ is the average ASA of randomly picked 200 structures. They are strongly correlated with $<A>$ values from 23 proteins[11] and 35 proteins.[21]
[d]Volume-corrected transfer free energy from octanol to water.[8]
[e]The estimated standard deviation (from program lfit[37]).
[f]Hydrophobic residues.

for Cys and $R > 0.88$ for other 19 residues.) The regression intercepts for all 20 residues are similar in magnitude (1.9 kcal/mol for Cys and 0.4–1.4 kcal/mol for the rest). This is because fully exposed side-chains do not interact strongly with the rest of proteins (except the bonded part); thus, their contributions to stability will not strongly depend on the details of their side-chains. However, the regression slopes are very different. For example, Figure 3 shows the APMF results of Leu and Thr. A hydrophobic residue (Leu) has a much steeper slope than a hydrophilic residue (Thr) does. We shall call the slope the buriability $B(I)$ of an amino acid residue (Table I) because it is the change in stability as buried area increases. This parameter provides a quantitative measure of the driving force for the burial of a residue. The results from mutations, on the other hand, yielded fewer and more scattered data points [ΔG_m(I), Fig. 3]. Only five residues (Tyr, Phe, Met, Ala, and Thr) have a strong correlation ($R > 0.7$) with a correlation slope in a good quantitative agreement with that from APMF. A larger mutation database is clearly needed for more accurate comparison. It is of interest to note that $\Delta G_s(I)$ obtained from other two all-atom knowledge-based potentials[12,13] have much weaker or no significant correlation with A^0–$<A>$ for hydrophilic residues (Table II). This

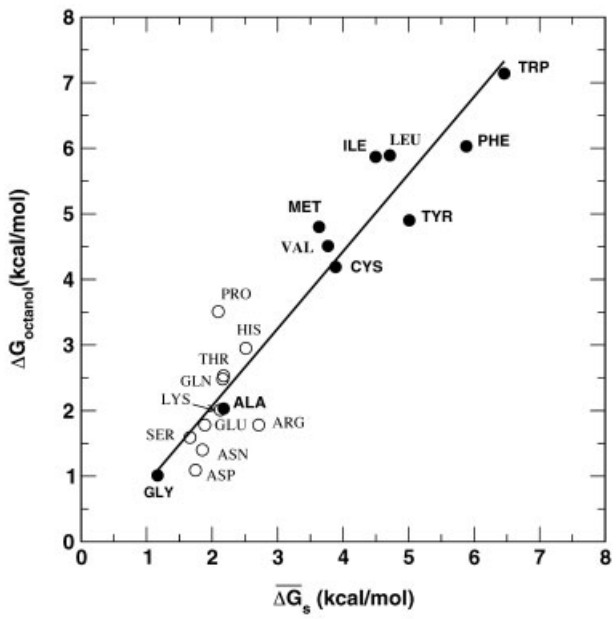

Fig. 1. The correlation between the corrected octanol to water transfer free energy and $\overline{\Delta G_s}$. The line is regression line for all residues. There is no significant correlation for hydrophilic residues ($R = 0.51$, open circles).

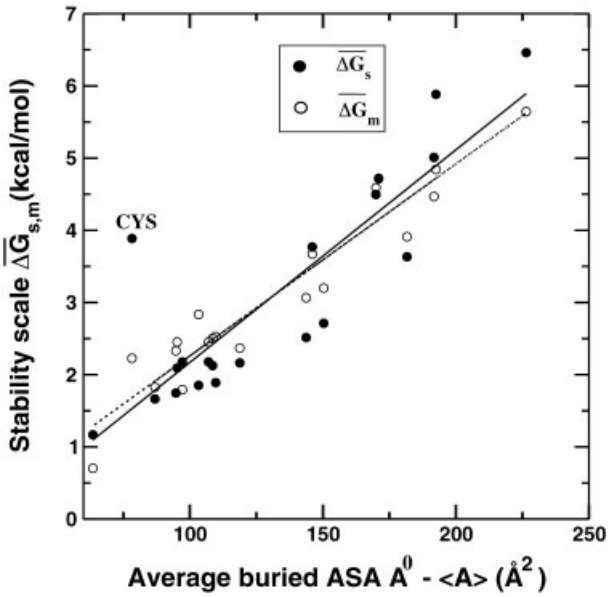

Fig. 2. Significant correlations are observed between the average buried accessible surface area (A^0–<A>) and the new stability scales ($\overline{\Delta G}_s$ in filled and $\overline{\Delta G}_m$ in open circles). For $\overline{\Delta G}_s$, there is an obvious outlier (Cys). This is perhaps due to inability of the knowledge-based potential to describe accurately the formation of disulfide bonds. The correlation coefficient is 0.95 without Cys. For $\overline{\Delta G}_m$, R = 0.96. The lines are from regression analysis.

TABLE II. Correlation Coefficients Between the Buried ASA and the Average Contribution of a Residue to the Stability of a Protein (ΔG_s) for Three Different APMF

Residue	RAPDF[a]	Atomic KBP[b]	DFIRE[c]
Trp	0.63	0.83	0.90
Tyr	0.70	0.86	0.94
Phe	0.55	0.81	0.90
Ile	0.61	0.80	0.91
Leu	0.71	0.86	0.95
Met	0.48	0.78	0.88
Val	0.70	0.86	0.94
Ala	0.54	0.89	0.97
Cys	0.26	0.63	0.79
His	0.43	0.46	0.90
Arg	0.34	−0.70	0.90
Gln	0.28	−0.88	0.93
Glu	0.51	−0.90	0.92
Thr	0.55	0.46	0.95
Asn	0.28	−0.89	0.95
Lys	0.07	−0.93	0.88
Pro	−0.10	−0.76	0.96
Ser	0.35	−0.57	0.95
Asp	0.55	−0.94	0.94
Gly	−0.37	0.43	0.96

[a]Ref. 12.
[b]Ref. 13.
[c]Ref. 6.

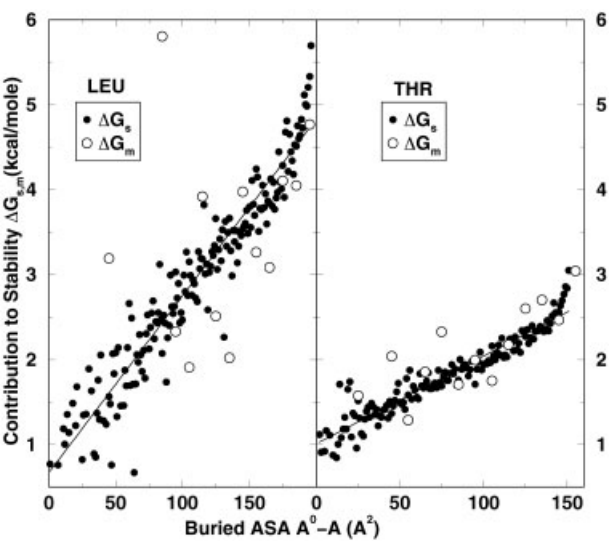

Fig. 3. The contribution of Leu and Thr to stability as a function of their buried accessible surface area (A^0–A). Both results from APMF (in filled circles) and mutation data (in open circles) are shown. Lines are from linear regression of APMF results. R =0.95 and 0.95 for Leu and Thr, respectively. In this figure, to have a clear comparison of the slope (buriability), ΔG_m (Thr) was shifted slightly downward because $\overline{\Delta G}_m$(Thr) is slightly higher than $\overline{\Delta G}_s$(Thr) (Table I). $\overline{\Delta G}_m$(Leu) was not shifted.

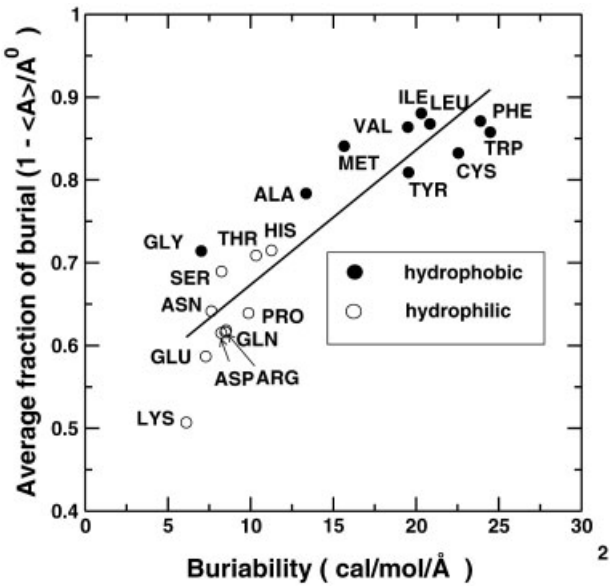

Fig. 4. The buriability of amino acid residues versus the average fractions of buried accessible surface area of 20 amino acid residues from 200 soluble proteins (1 − <A>/A^0). R = 0.91, 0.86, and 0.84 for all, hydrophobic (filled circles), and hydrophilic (open circles) residues, respectively. Line is from linear regression of 20 residues.

result further distinguishes the new DFIRE-based APMF from previously developed methods (see Discussion).

Buriability reproduces the fact that hydrophobic residues tend to be buried in soluble proteins. It has a significant correlation with the average fraction of buried accessible surface area (ASA) (1–<A>/A^0, also called burial propensity[14]), which is the probability that a particular type of a residue is buried calculated from a database of 200 protein structures (see Table I and Fig. 4). R = 0.91, 0.86, and 0.84 for all 20 residues, hydrophobic, and hydrophilic residues, respectively. In contrast, there is no statistically significant correlation between hydrophilic portions of 1–<A>/A^0 and the measured transfer free energy

$\Delta G_{octanol}$. Thus, hydrophobic residues are buried because their burial will lead to a larger gain in stability than the burial of hydrophilic residues. Figure 4 shows a large gap between the buriability of hydrophilic residues and those of hydrophobic residues (except the smallest residue Gly). The average buriability of hydrophilic residues is 10.1 cal $mol^{-1}Å^{-2}$ lower than that of hydrophobic residues.

DISCUSSION

In this article, two totally different approaches were used to characterize the contributions of individual residues to folding stability. The knowledge-based APMF, which was derived with a physical ideal-gas reference state and the fundamental equations of statistical mechanics,[6] can provide a reasonably accurate prediction of the mutation-induced change in stability.[6] The APMF does not take into account the contributions of backbone entropy,[6,15] multiple-body effects of solvation,[16] and the structures of denatured states[17,18] and possible other terms.[19] These effects either cannot be dissected into the contribution of individual residues (thus are not important for the purpose of this article) or are taken into account implicitly in the mutation approach. The latter extracted the average contribution to stability of an amino acid residue using experimentally measured stabilities as input. Therefore, the good agreement between the results of stability scale obtained from the mutation database and that from APMF support the overall picture presented here. However, more quantitative comparison on buriability will require a substantially large mutation database so that there are sufficient mutation data on different values of buried ASA.

The stability scale obtained from APMF and mutation data has a significant correlation with the average buried ASA for both hydrophobic and hydrophilic portions of the scales. However, it only correlates with hydrophobic portion of many water-to-oil transfer scales including the new scale from Jayasinghe et al.[20] This is true whether the backbone contribution to stability is removed in our calculations because the backbone contribution is more or less a constant, as expected. The result suggests that organic solvent is not a good approximation as the interior of proteins for hydrophilic residues,[21] as indicated by the fact that different solvents produce different scales for hydrophilic residues.[22,23]

There is a question regarding whether the positive linear correlation between the contribution to stability and buried ASA has resulted from trivial consequence of statistical analysis of structural database. Intuitively, more burial means more contacts and, therefore, higher APMF. We found that although it is true that more burial means more contacts, more contacts do not always lead to higher APMF. This is because APMF is obtained from the number of contacts (N_{obs}) relative to the number of contacts in the reference state (N_{exp}). It is possible that although the number of contacts increases as a residue is buried deeper, the increment may be smaller than the increment from the number of contacts in the reference state. The latter will yield a lower APMF as buried ASA increases. Figure 5 illustrates one example from atomic KBP potential[13] for residue Asn where the APMF potential leads to a significant negative correlation between the contribution to stability and buried ASA (anti-burial) [Fig. 5B], despite the fact that the average number of contacts for reference state and that observed from protein structures both increase as buried ASA increases. Figure 5 also shows that the contribution to stability, ΔG_s (=fRT $\overline{\ln N_{obs}}$ − $fRT\,\overline{\ln N_{exp}}$) is only about 2% of the value of either $fRT\,\overline{\ln N_{exp}}$ or $fRT\,\overline{\ln N_{obs}}$. Thus, APMF is very sensitive to small changes in the reference state.[6] In fact, among three knowledge-based potentials (RAPDF,[12] atomic KBP,[13] and DFIRE), DFIRE is the only method that has consistently significant positive correlation (Table II). There are many residues whose correlations between the buried ASA and the average contribution of a residue to the stability of a protein (ΔG_s) are insignificant for the RAPDF method. Negative and insignificant correlations are found for some hydrophilic residues in the atomic KBP. Thus, the observa-

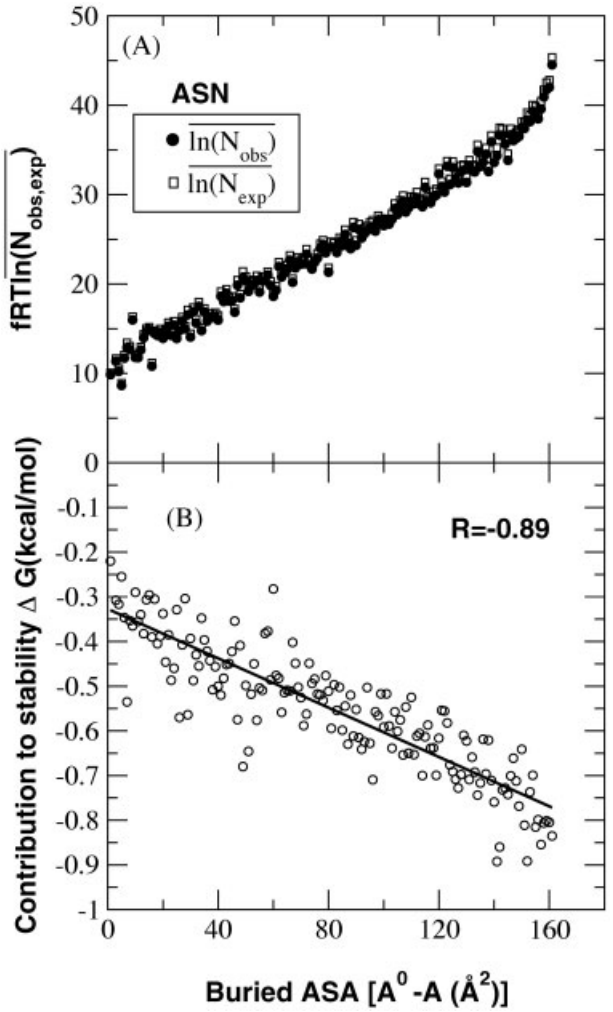

Fig. 5. **A:** $fRT\,\overline{\ln N_{obs}}$ and $fRT\,\overline{\ln N_{exp}}$ for Asn as a function of buried ASA obtained from APMF by atomic KBP method. **B:** The contribution of residue Asn to stability as a function of the buried accessible surface area (A^0–A) for the same method. The solid line is from linear regression of the APMF results.

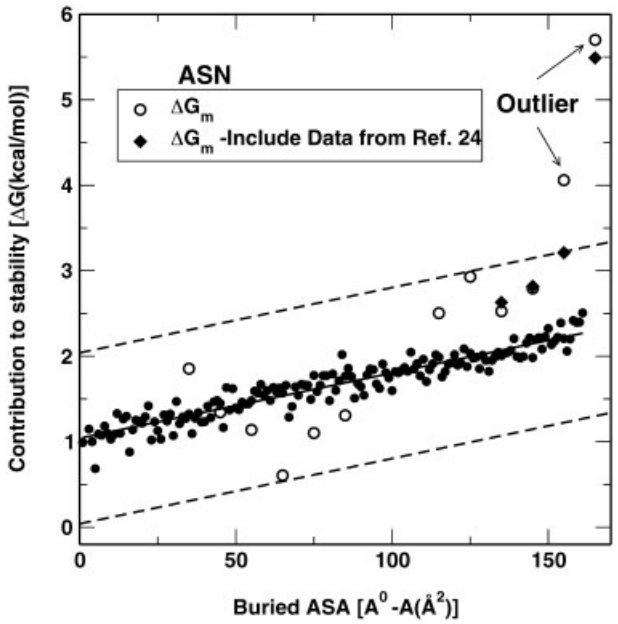

Fig. 6. The contribution of residue Asn to stability as a function of the buried accessible surface area (A^0–A). Results from DFIRE-based APMF (ΔG_s, in filled circles) and mutation data (ΔG_m, in open circles) are shown. The solid line is from linear regression of the APMF results ($R = 0.95$). The dashed lines denote the upper and lower boundaries of 1 kcal/mol from the regression line. The filled diamond is ΔG_m after the inclusion of mutation results for highly buried Asn listed in Ref. 24.

tion of positive correlation in DFIRE-based APMF is a nontrivial result.

Buriability suggests that the burial of hydrophilic residues contribute less to stability than the burial of hydrophobic residues. This is the result based on analyzing 200 known structures using DFIRE-based APMF as well as the approximate result extracted from mutations. However, this finding appears to contradict the recent work by Pace[5] who made an opposite conclusion based on eight mutations of mostly buried Asn to Ala. To understand the origin of this discrepancy, we show the contribution of residue Asn to stability as a function of the buried ASA in Figure 6. Most data points from mutation agree with the APMF results within 1 kcal/mol boundary. The most significant outlier (at the highest buried ASA) was the result extracted from only one mutation involving Asn, whereas the other significant outlier (at the second highest buried ASA) was from only two mutations. These two outliers appear to agree more with Pace's statement that polar group burial contributes more to protein stability than nonpolar group burial. Because the number of mutations at these two points are too small, we added eight Asn to Ala mutations as well as five Asn to Ser and Asp mutations to our database (Table 5 of Ref. 24). This produces three and six more mutations for extraction at the highest and the second highest burial ASA, respectively. The total number of mutations for extracting ΔG_m^{ASN} are four and eight mutations at the highest and the second highest burial ASA, respectively. It is of interest that the inclusion of more experimental data makes the outlier at the second highest burial ASA within 1 kcal/mol boundary from the APMF regression line. The value at the highest burial ASA also shifts slightly downward. This finding suggests that the conclusion of larger stability contribution from polar group than from hydrophobic group by Pace heavily depended on the mutation data at 100% burial. Indeed, there are two Asn to Ala mutations at 100% burial that causes a change of 5 kcal/mol in stability. This number is significantly >1.7–2.9 kcal/mol for six other mutation data. It is not yet certain if the significant spike at 100% burial shown in Figure 6 is due to a small number of data points or reflected something more fundamental, as suggested by Pace. Nevertheless, the agreement between APMF results and the results from mutation data is reasonable at all other smaller percentages of burial.

The buriability scale obtained here is contributed by both residue–residue and residue-solvent interactions. Thus, it does not provide specific evidence for supporting either a hydrophobic model or a packing model for protein stability. Rather, it suggests a combination of the two models. On one hand, buriability has a significant correlation with the corrected octanol-to-water transfer scale.[8] $R = 0.92$, 0.89, and 0.68 for all 20 residues, hydrophobic, and hydrophilic residues, respectively. This finding suggests that hydrophobicity plays an important role in determining buriability. On the other hand, we also found a significant correlation between buriability and the melting points of the crystals of 20 amino acids[25] ($R = 0.66$ with a p value of 1.5×10^{-3}). The melting point of an amino acid represents the overall stability of its solid phase or the overall strength of its packing interaction with itself in the absence of solvent. Moreover, it was shown that the composition in the core of membrane proteins is similar to that of soluble proteins, and the solvent effect of hydrophobic lipid bilayers is limited to the composition on the surface of membrane proteins.[26] Thus, the intrinsic property of an amino acid residue, in addition to its hydrophobicity, also affects its buriability.

There is an intrinsic difference between polar/charged and nonpolar interactions, which contributes to high buriability of hydrophobic residues. Polar interactions are orientationally dependent; thus, specific ordering is required for energy-optimized burial. For charged residues, the tendency to make a specific salt bridge for energy minimization also makes burial in the interior more difficult. The same restriction does not apply to hydrophobic residues because their interactions are isotropic. Water is a good example to illustrate the difficulty of the packing (or deep burial) of polar molecules. The density of ice has to be decreased to satisfy hydrogen bonding. In addition, it has been shown that the volume of polar residues increases, whereas that of nonpolar residues decreases on folding.[3] Moreover, Gekko and Noguchi[27] found that water around nonpolar groups has greater compressibility than water around polar and charged groups. Their results suggest that even with water, nonpolar groups are more packable (thus, higher buriability) than polar and charged ones.

The large buriability gap between hydrophobic and hydrophilic residues may also be contributed by the struc-

tural difference among 20 natural amino acid residues. All side-chains of hydrophilic residues are made of linear alkanes, whereas side-chains of hydrophobic residues can be made of linear or branched alkanes, or of aromatic groups. Charged residues Lys and Arg have the longest linear portions of side-chains (5 heavy atoms) among 20 amino acids. In contrast, the longest linear portion of hydrophobic side-chains (except Met) is only two. (The linear portion of side-chains is defined as the portion of a side-chain that has no branch except the last heavy atom.) The aromatic group in some hydrophobic residues also makes their side-chains more isotropically accessible. In other words, hydrophobic residues are entropically more favorable for burial. Indeed, an empirical scale for the loss of side-chain conformational entropy developed by Pickett and Sternberg[28] showed a marked difference between hydrophobic and hydrophilic residues. The average loss of entropy for nine hydrophobic residues (except Gly) is 0.76 kcal/mol, whereas the corresponding number for nine hydrophilic residues (except Pro) is 1.67 kcal/mol. Thus, we speculate that the shapes of naturally occurring hydrophilic residues were evolutionally optimized to enhance anisotropy of their interactions, whereas the opposite is true for hydrophobic residues. That is, evolution of natural amino acid residues seems to facilitate the tight and strong packing of hydrophobic residues while making the burial of hydrophilic residues inside the dense core of proteins more difficult. One possible explanation is that evolution optimizes for solubility, which requires the surface of globular proteins to be made of mostly hydrophilic residues. However, shape is certainly not the only factor that determines buriability. For example, the buriability of hydrophilic Arg is larger than the other two hydrophilic residues Asp and Asn although the former has a longer chain than either Asp or Asn. More studies are certainly needed to further address these issues.

The buriability parameter with a built-in partitioning of hydrophilic and hydrophobic residues offers a simple residue-based potential for folding and binding studies. Possible applications include structure selections from decoys, structure prediction, and predictions of mutation-induced change in stability. The use of the buriability parameter has led to an efficient, accurate folding recognition method called SPARKS (http://theory.med.buffalo.edu).[29]

METHODS

Extracting Atom–Atom Potential of Mean Force

A knowledge-based atom–atom potential of mean force (APMF) $\bar{u}(i, j, r)$ between atom types i and j that are distance r apart is all extracted from a common equation given by

$$\bar{u}(i,j,r) = \begin{cases} -fRT \ln \dfrac{N_{\text{obs}}(i,j,r)}{N_{\text{exp}}(i,j,r)}, & r < r_{\text{cut}}, \\ 0, & r > r_{\text{cut}}, \end{cases} \qquad (1)$$

where f is a constant scaling factor, R is the gas constant, $T = 300\text{K}$, $N_{\text{obs}}(i, j, r)$ is the number of (i, j) pairs within the distance shell r observed in folded proteins, and $N_{\text{exp}}(i, j, r)$ is the expected number of atomic pairs (i, j) in the same distance shell if there were no interactions between atoms (the reference state). Clearly, an accurate description of the zero-interaction reference state is required to obtain the net effect of residue–residue and residue-solvent interactions.

In a recent article, we used a distance-scaled, finite ideal-gas state as the reference state[6] in which the expected number of atomic pairs $N_{\text{exp}}(i, j, r)$ satisfies

$$N_{\text{exp}}(i,j,r) = \left(\frac{r}{r_{\text{cut}}}\right)^{\alpha}\left(\frac{\Delta r}{\Delta r_{\text{cut}}}\right)N_{\text{obs}}(i,j,r_{\text{cut}}) \qquad (2)$$

where $r_{\text{cut}} = 15$ Å, and $\Delta r/\Delta r_{\text{cut}}$ is the correction factor for different bin widths at r and r_{cut}. For a detailed derivation, see Ref. 6. Although α is equal to 2 exactly for an infinite ideal-gas system, we found that setting α to 1.61 is best suited for finite proteins.[6] The potential was generated by using a nonhomologous (<30% homology) structural database of 1011 soluble proteins with resolution < 2 Å.[30] Residue-specific atomic types were used (167 atomic types).[12,13] The bin width $\Delta r = 2$ Å, for $r < 2$ Å; = 0.5 Å for 2 Å $< r <$ 8 Å; = 1 Å for 8 Å $< r <$ 15 Å. The constant scaling factor was determined so that the regression slope between predicted and experimentally measured changes in stability due to mutation is equal to 1.[6] The constant prefactor f is needed because temperature is a free parameter in knowledge-based potentials derived from static structures.

The new potential was shown to recognize more native proteins from multiple decoy sets and provide more accurate prediction of mutation-induced changes in protein stability than two previously developed, residue-specific, all-atom knowledge-based potentials.[12,13] The latter used a statistically averaged reference state.[31] On the other hand, the new reference state (Eq. 2) is based on a noninteracting ideal-gas reference state commonly used in liquid-state statistical mechanical theories.[32] This physical reference state unifies the structure-derived potential of mean force for folding and binding studies,[33] as indicated by the successful direct application of this "monomer" potential for prediction of binding free energy and selection of native complex structures from docking decoys.

Stability Scale and Buriability

The stability contribution of each residue (stability scale) was calculated from APMF as follows:

$$\overline{\Delta G}_s(I) = \langle \Delta G_s(I) \rangle = -\left\langle \frac{1}{2} \sum_{i \in I, j \notin I} \bar{u}(i,j,r_{ij}) \right\rangle \qquad (3)$$

where the summation is over all the pairs between atom i of residue I and atom j of other residues, <> denotes the average over all residue type "Is" of proteins, and a negative sign in Eq. 3 was used to make a positive value as stabilizing. Here a factor of 1/2 is used so that the contribution of each pair to the total potential $[-\Sigma_I n_I \overline{\Delta G}_s(I)$ with n_I, the number of residue $I]$ is counted only once.[34] This results in a prefactor f of 0.0314. (This value is

doubled from 0.0157 used in Ref. 6 as the result of 1/2 in Eq. 3.) We only used 200 randomly selected structures from the 1011 protein structures for the calculations of $\Delta G_s(I)$ to reduce the computational requirement for evaluating accessible surface. Increasing the number of structures yielded essentially the same scale. The accessible surface area (ASA) of a residue was calculated by the Lee-Richards algorithm with 1.4 Å probe.[35] The buried ASA is equal to $A^0 - A$ where A^0 is the solvent accessible area of the unfolded state due to Shrake and Rupley.[36]

The dependence of the stability contribution on the buried ASA, $A^0 - A$, was obtained by calculating the buried ASA and the contribution to total APMF for each residue of a protein, $\Delta G_s(I)$. The results were averaged over a 1 Å^2 bin. Buriability is defined as the slope determined by linear regression.

Mutation-Based Results

We extracted $\overline{\Delta G}_m$ from mutation data by minimizing the quantity s, which is defined by

$$s = \sum (\Delta\Delta G_{\text{exp}} + \Delta\Delta G_m)^2 \qquad (4)$$

where $\Delta\Delta G_{\text{exp}}$ is from experimentally measured change in free energy [$= \Delta G(\text{mutant}) - \Delta G(\text{wild})$], $\Delta\Delta G_m(I \rightarrow J) = \overline{\Delta G}_m(J) - \overline{\Delta G}_m(I)$ with $\overline{\Delta G}_m(J)$, the average free energy of transfer of residue J from protein interior to water. The minimization was done by the simple linear least squares fitting method. (The term linear refers to the linear relation between the fitting parameter and data to be fitted.)[37] Because only relative values are entered in Eq. 4, we set $\overline{\Delta G}_m(\text{Gly}) = 0$ in order to determine the values for other residues. That is, there are 19 free parameters. A database of 1023 large to small point mutations of 35 proteins was collected to extract $\overline{\Delta G}_m$. The database contains 7 all-α, 7 all-β, and 21 mixed α/β proteins. The values of pairwise sequence identity are <20% for the top 10 proteins, each of which have >30 mutations. The details can be found in Ref. 21, and a complete list of 1023 mutations is shown in http://theory.med.buffalo.edu

The dependence of ΔG_m as a function of burial ASA was obtained by grouping $I \rightarrow X$ mutations based on the value of buried ASA of residue I with a bin width of 10 Å^2. A smaller mutation database was constructed by one group of $I \rightarrow X$ mutations and the mutations that do not involve residue I. The result of $\overline{\Delta G}_m(I)$ from the smaller database is one data point in the plot of $\Delta G_m(I)$ versus burial ASA.

ACKNOWLEDGMENTS

We thank Professors Martin Karplus, Robert Baldwin, Themis Lazaridis, Hue Sun Chan, Richard Cheng, Apichart Linhananta, and reviewers for their critical reading, helpful comments, and discussion.

REFERENCES

1. Kauzmann W. Some factors in the interpretation of protein denaturations. Adv Protein Chem 1959;14:1–63.
2. Dill KA. Dominant forces in protein folding. Biochemistry 1990;29: 7133–7155.
3. Harpaz Y, Gerstein M, Chothia C. Volume changes on protein folding. Structure 1994;2:641–649.
4. Ratnaparkhi GS, Varadarajan R. Thermodynamic and structural studies of cavity formation in proteins suggest that loss of packing interactions rather than the hydrophobic effect dominates the observed energetics. Biochemistry 2000;39:12365–12374.
5. Pace CN. Polar group burial contributes more to protein stability than nonpolar group burial. Biochemistry 2001;40:310–313.
6. Zhou H, Zhou Y. Distance-scaled, finite ideal-gas reference state improves structure- derived potentials of mean force for structure selection and stability prediction. Protein Sci 2002;11:2714–2726. Corrections 2003;12:2121.
7. Fauchere JL, Pliska V. Hydrophobic parameters 1/4 of amino acid side chains from the partitioning of n-acetylamino-acid amides. Eur J Med Chem 1983;18:369–375.
8. Sharp KA, Nicholls A, Friedman R, Honig B. Extracting hydrophobic free energies from experimental data: relationship to protein folding and theoretical models. Biochemistry 1991;30:9686–9697.
9. Tanford C. The hydrophobic effect: formation of micelles and biological membrances. New York: Wiley; 1980.
10. Chothia C. The nature of the accessible and buried surfaces in proteins. J Mol Biol 1976;105:1–14.
11. Rose GD, Geselowitz AR, Lesser GJ, Lee RH, Zehfus MH. Hydrophobicity of amino acid residues in globular protein. Science 1985;229:834–838.
12. Samudrala R, Moult J. An all-atom distance-dependent conditional probability discriminatory function for protein structure prediction. J Mol Biol 1998;275:895–916.
13. Lu H, Skolnick J. A distance-dependent atomic knowledge-based potential for improved protein structure selection. Proteins 2001; 44:223–232.
14. Zhou H, Zhou Y. Predicting the topology of transmembrane helical proteins using mean burial propensity and a hidden-Markov-model-based method. Protein Sci 2003;12:1547–1555.
15. Lazaridis T, Karplus M. Effective energy function for protein structure prediction. Curr Opin Struct Biol 2000;10:139–145.
16. Shimizu S, Chan HS. Anti-cooperativity in hydrophobic interactions: a simulation study of spatial dependence of three-body effects and beyond. J Chem Phys 2001;115:1414–1421.
17. Pakula AA, Sauer RT. Reverse hydrophobic effects relieved by amino-acid substitutions at a protein surface. Nature 1990;344: 363–364.
18. Klein-Seetharaman J, Oikawa M, Grimshaw SB, Wirmer J, Duchardt E, Ueda T, Imoto T, Smith LJ, Dobson CM, Schwalbe H. Long-range interactions within a nonnative protein. Science 2002; 295:1719–1722.
19. Brem R, Chan HS, Dill KA. Extracting microscopic energies from oil-phase solvation experiments. J Phys Chem B 2000;104:7471–7482.
20. Jayasinghe S, Hristova K, White SH. Energetics, stability, and prediction of trans-membrane helices. J Mol Biol 2001;312:927–934.
21. Zhou H, Zhou Y. The stability scale and atomic solvation parameters extracted from 1023 mutation experiments. Proteins 2002;49: 483–492.
22. Karplus PA. Hydrophobicity regained. Protein Sci 1997;6:1302–1307.
23. Chan HS. Amino acid side-chain hydrophobicity. In: Encyclopedia of Life Sciences. D. Atkins, ed. London: Nature Publishing Group; 2001.
24. Hebert EJ, Giletto A, Jozef Sevcik LU, Wilson KS, Dauter Z, Pace CN. Contribution of a conserved asparagine to the conformational stability of ribonucleases Sa, Ba, and T1. Biochemistry 1998;37: 16192–16200.
25. Weast RC, Astle MJ. CRC handbook of data on organic compounds. Boca Raton, FL: CRC Press; 1985.
26. Rees DC, DeAntonio L, Eisenberg D. Hydrophobic organization of membrane proteins. Science 1989;245:510–513.
27. Gekko K, Noguchi H. Hydration behavior of ionic dextram derivatives. Macromolecules 1974;7:224–229.
28. Pickett SD, Sternberg MJ. Empirical scale of side-chain conformational entropy in protein folding. J Mol Biol 1993;231:825–839.
29. Zhou H, Zhou Y. Single body knowledge-based energy score combined with sequence-profile and secondary structure information for fold recognition. Proteins 2004; in press.
30. Hobohm U, Scharf M, Schneider R, Sander C. Selection of representative protein data sets. Protein Sci 1992;1:409–417.
31. Sippl MJ. Calculation of conformational ensembles from potentials of mean force. An approach to the knowledge-based predic-

tion of local structures in globular proteins. J Mol Biol 1990;213: 859–883.
32. Friedman HL. A course in statistical mechanics. Englewood Cliffs, NJ: Prentice-Hall, Inc.; 1985.
33. Liu S, Zhang C, Zhou H, Zhou Y. A physical reference state unifies the structurederived potential of mean force for protein folding and binding. Proteins 2004; in press.
34. Norel R, Sheinerman F, Petrey D, Honig B. Electrostatic contributions to protein-protein interactions: fast energetic filters for docking and their physical basis. Protein Sci 2001;10: 2147–2161.
35. Lee B, Richards FM. The interpretation of protein structures: estimation of static accessibility. J Mol Biol 1971;55:379–400.
36. Shrake A, Rupley JA. Environment and exposure to solvent of protein atoms. Lysozyme and insulin. J Mol Biol 1973;79:351–371.
37. Press WH, Teukolsky SA, Vetterling WT, Flannery BP. Numerical recipes: the art of scientific computing. Cambridge: Cambridge University Press; 1989.
38. Casari G, Sippl MJ. Structure-derived hydrophobic potential. Hydrophobic potential derived from x-ray structures of globular proteins is able to identify native folds. J Mol Biol 1992;224:725–732.
39. Miyazawa S, Jernigan RL. Estimation of effective interresidue contact energies from protein crystal structures: quasi-chemical approximation. Macromole 1985;18:534–552.